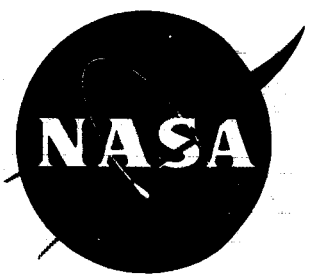


c. 1

NASA TN D-856



LOAN COPY: R  
AFSWC (S  
KIRTLAND A

TECH LIBRARY KAFB, NM  
0153319

# TECHNICAL NOTE

## D-856

EXPERIMENTAL EVALUATION OF ANALYTICAL MODELS FOR  
THE INERTIAS AND NATURAL FREQUENCIES OF FUEL  
SLOSHING IN CIRCULAR CYLINDRICAL TANKS

By Robert W. Warner and John T. Caldwell

Ames Research Center  
Moffett Field, Calif.

NATIONAL AERONAUTICS AND SPACE ADMINISTRATION  
WASHINGTON  
May 1961



NATIONAL AERONAUTICS AND SPACE ADMINISTRATION

TECHNICAL NOTE D-856

EXPERIMENTAL EVALUATION OF ANALYTICAL MODELS FOR  
THE INERTIAS AND NATURAL FREQUENCIES OF FUEL  
SLOSHING IN CIRCULAR CYLINDRICAL TANKS

By Robert W. Warner and John T. Caldwell

## SUMMARY

A correlation is presented of experimental measurement and analytical prediction of free, planar oscillations of a tank of mercury hung on a pendulum. Measured frequencies are presented for the slosh mode and the pendulum-tank mode, and time-history wave forms are included for qualitative comparisons. The sloshing is represented analytically by a single pendulum or a spring-bob, and the size and location of their inertias are determined by matching forces and moments on the tank surface with linearized hydrodynamic theory for inviscid fluids. It is concluded that such analytical models are identical for small displacements in the present application (as they are in simpler applications) and that they provide excellent simulation of the stiffness and inertia terms for fuel sloshing.

## INTRODUCTION

A severe aero-servo-elastic stability problem can occur for vehicles which have a flexible structure and a swivelling rocket motor with high-gain control response. In an analytical study of such a problem fuel sloshing can be important as long as appreciable liquid fuel remains unburned. It is then necessary to determine whether the sloshing has a direct effect on stability, an indirect effect by modification of a deformation pattern, or no effect at all. Such an analytical study is often facilitated when the fuel sloshing is incorporated in terms of analytical models, specifically pendulums or spring-bobs. Hence the main purpose of the present report is to evaluate experimentally the accuracy of these analytical models for a portion of the fuel sloshing problem, namely, the stiffness and inertia terms for sloshing in circular cylindrical tanks undergoing oscillations in a plane. A secondary purpose is to compare the pendulum and spring-bob models.

A great deal of work has been done on sloshing of fluids in containers, and reference 1 is an excellent survey with an extensive bibliography. Guthrie (ref. 2) and Rayleigh (ref. 3) provided one of the earliest correlations between experiment and theory, showing excellent agreement as to fluid natural frequency. These results, however, are for stationary tanks.

An extensive correlation on the frequency response of the fluid force on the wall of an oscillating tank can be found in references 4 to 7. Among these references there are comparisons of experiment and theory for high-damping tank configurations with baffles and low-damping configurations with bare tank walls. It is worthwhile to focus attention on the off-resonance correlations and the natural frequencies for the low-damping frequency responses (appearing in refs. 5-7) in order to evaluate errors in the stiffness and inertia simulation with minimum effect of the errors in the damping simulation. On that basis, references 5 to 7 indicate generally satisfactory stiffness and inertia simulation for the fluid force on the tank wall. Unfortunately, there are no moments measured on the surface of the tanks in references 5 to 7.

The present experimental evaluation is based on low-amplitude, free, planar oscillations of a small, smooth-walled tank of mercury hung on a pendulum (the weight ratio of the mercury to the present rigid tank being representative of actual missiles, in which the fuel can be massive enough to have a significant effect). This test setup is simulated mathematically by linearized equations of motion for an undamped two-degree-of-freedom system, with fuel sloshing represented by a single pendulum or a spring-bob. Solutions are compared with the experimental oscillations in terms of frequencies and wave forms. These measured and predicted quantities should be significantly affected by the fluid moments on the tank surface. Small amplitudes and linearized equations are used throughout for simplicity since oscillations universally begin at low amplitude unless an artificial initial condition is applied.

Simple analytical models for fuel sloshing have also received a great deal of attention. Reference 8 shows that a system with spring-bobs and a fixed mass and rotary inertia exactly duplicates the tank-surface forces and moments given by linearized hydrodynamic theory for a rectangular tank oscillating in lateral translation, pitch, and yaw. References 6 and 9 present similar exact systems for a cylindrical tank.

The historical development of the pendulum model has not been as free of error as that of the spring-bob model. Reference 3 gives the correct lengths for pendulums which match the experimental and theoretical fluid natural frequencies. Reference 10, however, presents pendulum masses based on duplicating the fluid force given by hydrodynamic theory on the wall of a rectangular tank restricted to zero motion. Unfortunately, the case of a stationary tank is not suitable for determining the pendulum masses, being useful only for finding the relative magnitudes of initial conditions for a fluid mode and its pendulum model after the masses have already been determined by another method. The correct pendulum masses and pivot-point locations for a cylindrical tank, plus the magnitude and location of a fixed mass and the magnitude of its rotary inertia, can be found among references 11 to 13, as derived on the basis of forces and moments on the surface of a tank undergoing forced lateral and pitching oscillations.

As a result of the history just cited for the pendulum model, it appeared useful to compare the relationship of the pendulum model to the spring-bob model. For completeness, a brief development of the two models is given in the appendix prior to their comparison.

#### NOTATION

A	infinite summation defined in equation (A5)
a	interior radius of tank
b	effective gravity
cg	center of gravity
e	Naperian base
$\left. \begin{matrix} F_x \\ F_{xp} \end{matrix} \right\}$	total fluid force on the wall of a tank undergoing forced lateral oscillations, as determined by hydrodynamic theory and the pendulum model, respectively; positive right
$\left. \begin{matrix} F_{xnp} \\ F_{xns} \end{matrix} \right\}$	that part of the fluid force on the wall of a tank undergoing forced lateral oscillations which is contributed by the nth pendulum and the nth spring-bob, respectively; positive right, $n = 1, 2, \dots, N$
$\left. \begin{matrix} F_{xop} \\ F_{xos} \end{matrix} \right\}$	that part of the fluid force on the wall of a tank undergoing forced lateral oscillations which is contributed by the fixed mass in the pendulum model and the spring-bob model, respectively; positive right
$\left. \begin{matrix} F_\theta \\ F_{\theta p} \end{matrix} \right\}$	total fluid force on the wall of a tank undergoing forced pitching oscillations (about the center of gravity of the undisturbed fluid), as determined by hydrodynamic theory and the pendulum model, respectively; positive right
$\left. \begin{matrix} F_{\theta np} \\ F_{\theta ns} \end{matrix} \right\}$	that part of the fluid force on the wall of a tank undergoing forced pitching oscillations (about the center of gravity of the undisturbed fluid) which is contributed by the nth pendulum and the nth spring-bob, respectively; positive right, $n = 1, 2, \dots, N$
$\left. \begin{matrix} F_{\theta op} \\ F_{\theta os} \end{matrix} \right\}$	that part of the fluid force on the wall of a tank undergoing forced pitching oscillations (about the center of gravity of the undisturbed fluid) which is contributed by the fixed mass in the pendulum model and the spring-bob model, respectively; positive right

4

- $h$  fluid height
- $I$  mass moment of inertia of the empty pendulum tank about its pivot point
- $I_{op}$  } mass moment of inertia of the fixed mass about its own center  
 $I_{os}$  } of gravity in the pendulum model and the spring-bob model, respectively
- $I_o$  common symbol for  $I_{op}$  and  $I_{os}$  after they are proved equal
- $k_n$  total spring stiffness acting on the  $n$ th mass in the spring-bob model,  $n = 1, 2, \dots, N$
- $L_n$  length of the  $n$ th simple pendulum in the pendulum model,  $n = 1, 2, \dots, N$
- $l$  shortest distance from the hinge line to the center of gravity of the empty pendulum tank
- $l_m$  shortest distance from the hinge line of the pendulum tank to the center of gravity of the undisturbed fluid
- $l_{fp}$  } shortest distance, positive downward, from the hinge line of the  
 $l_{fs}$  } pendulum tank to the hinge line of the pendulum in the single-pendulum model and the attachment line of the spring in the single-spring-bob model, respectively
- $l_t$  shortest distance, positive downward, from the hinge line of the pendulum tank to the center of gravity of the fixed mass in either the single pendulum or the single-spring-bob model
- $l_{np}$  } shortest distance, positive downward, from the center of gravity  
 $l_{ns}$  } of the undisturbed fluid to the hinge line of the  $n$ th pendulum in the pendulum model and the attachment line of the  $n$ th spring in the spring-bob model, respectively,  $n = 1, 2, \dots, N$
- $l_{op}$  } shortest distance, positive downward, from the center of gravity  
 $l_{os}$  } of the undisturbed fluid to the attachment line of the fixed mass in the pendulum model and the spring-bob model, respectively
- $l_o$  common symbol for  $l_{op}$  and  $l_{os}$  after they are proved equal
- $M$  mass of the empty pendulum tank
- $M_x$  } total fluid moment (about the center of gravity of the  
 $M_{xp}$  } undisturbed fluid) on the surface of a tank undergoing forced lateral oscillations, as determined by hydrodynamic theory and the pendulum model, respectively; positive clockwise

- $\left. \begin{array}{l} M_{xnp} \\ M_{xns} \end{array} \right\}$  that part of the fluid moment (about the center of gravity of the undisturbed fluid) on the surface of a tank undergoing forced lateral oscillations which is contributed by the  $n$ th pendulum and the  $n$ th spring-bob, respectively; positive clockwise,  $n = 1, 2, \dots, N$
- $\left. \begin{array}{l} M_{xop} \\ M_{xos} \end{array} \right\}$  that part of the fluid moment (about the center of gravity of the undisturbed fluid) on the surface of a tank undergoing forced lateral oscillations which is contributed by the fixed mass in the pendulum model and the spring-bob model, respectively; positive clockwise
- $\left. \begin{array}{l} M_{\theta} \\ M_{\theta p} \end{array} \right\}$  total fluid moment (about the center of gravity of the undisturbed fluid) on the surface of a tank undergoing forced pitching oscillations (about the same axis) as determined by hydrodynamic theory and the pendulum model, respectively; positive clockwise
- $\left. \begin{array}{l} M_{\theta np} \\ M_{\theta ns} \end{array} \right\}$  that part of the fluid moment (about the center of gravity of the undisturbed fluid) on the surface of a tank undergoing forced pitching oscillations (about the same axis) which is contributed by the  $n$ th pendulum and the  $n$ th spring-bob, respectively; positive clockwise,  $n = 1, 2, \dots, N$
- $\left. \begin{array}{l} M_{\theta op} \\ M_{\theta os} \end{array} \right\}$  that part of the fluid moment (about the center of gravity of the undisturbed fluid) on the surface of a tank undergoing forced pitching oscillations (about the same axis) which is contributed by the fixed mass with rotary inertia in the pendulum model and the spring-bob model, respectively; positive clockwise
- $m$  total mass of the fluid
- $\left. \begin{array}{l} m_{np} \\ m_{ns} \end{array} \right\}$  mass of the  $n$ th pendulum and the  $n$ th spring-bob, respectively,  $n = 1, 2, \dots, N$
- $m_n$  common symbol for  $m_{np}$  and  $m_{ns}$  after they are proved equal,  $n = 1, 2, \dots, N$
- $\left. \begin{array}{l} m_{op} \\ m_{os} \end{array} \right\}$  mass of the fixed fluid mass in the pendulum model and the spring-bob model, respectively
- $m_o$  common symbol for  $m_{op}$  and  $m_{os}$  after they are proved equal
- $N$  total number of pendulums or spring-bobs
- $n$  index indicating a specific mode or pendulum or spring-bob,  $n = 1, 2, \dots, N$  or  $\infty$

$n_s$	natural frequency of the slosh mode, that is, the mode which is mostly fuel motion, cps
$n_t$	natural frequency of the pendulum-tank mode, that is, the mode which is mostly tank motion, cps
$s_n$	lateral displacement of the mass of the $n$ th spring bob relative to the tank axis, positive right, $n = 1, 2, \dots, N$
$s_{xn}$	the $s_n$ type motion which results from lateral oscillations of the tank, $n = 1, 2, \dots, N$
$s_{\theta n}$	the $s_n$ type motion which results from pitching oscillations of the tank about the center of gravity of the undisturbed fluid, $n = 1, 2, \dots, N$
$t$	time, sec
$x$	lateral displacement of the tank in lateral translation; positive right
$x_0$	amplitude of $x$ in harmonic oscillation
$\epsilon_n$	$n$ th zero of $J_1'(\epsilon)$ , where $J_1(\epsilon)$ is the first-order Bessel function of the first kind and the prime indicates differentiation with respect to the argument, $n = 1, 2, \dots, \infty$
$\theta$	pitching displacement of the pendulum tank about its hinge line, or of the tank alone about the center of gravity of the undisturbed fluid
$\theta_0$	amplitude of $\theta$ in harmonic oscillation
$\phi_n$	pitching displacement of the $n$ th pendulum relative to the tank axis, positive clockwise, $n = 1, 2, \dots, N$
$\phi_{xn}$	the $\phi_n$ type motion which results from lateral oscillations of the tank, $n = 1, 2, \dots, N$
$\phi_{\theta n}$	the $\phi_n$ type motion which results from pitching oscillations of the tank about the center of gravity of the undisturbed fluid, $n = 1, 2, \dots, N$
$\omega$	circular frequency of forced harmonic oscillation, radians/sec
$\omega_n$	natural circular frequency of the $n$ th fluid mode, the $n$ th pendulum, or the $n$ th spring-bob, radians/sec, $n = 1, 2, \dots, N$ or $\infty$

## EXPERIMENTAL AND ANALYTICAL METHODS

### Apparatus and Test Technique

The experimental data were obtained with the model shown in figure 1. Basically it consisted of a 3.89-inch-inside-diameter tank mounted in a rigid frame and pivoted about a horizontal axis. The support arms could be moved along the longitudinal tank axis to vary the distance from the pivot point to the center of gravity of the empty tank. Mercury was used as the sloshing liquid.

Fluid surface displacement at the tank wall was measured with a cylindrical capacitive probe partially submerged in the liquid, and with an accompanying external bridge circuit. This measurement gave a time history of the fluid motion relative to the tank motion. Data for the tank motion were obtained with a noncontacting optical system. In this system a light beam is focused at a fixed point on the tank and through a servo control remains locked on the point for small tank displacements. The displacement of the light beam, which was proportional to the tank displacement, then activated a photoelectric cell and the output from the latter was recorded on an oscillograph. Similarly, the capacitive bridge circuit output, which was proportioned to the relative fluid motion, was recorded on an oscillograph.

In general, oscillations were initiated by pulling the tank to one side, allowing all fluid motion to cease, and then releasing the tank. For accuracy in determining the slosh mode frequency, the mode was excited by manually forcing the tank at a frequency near that of the slosh mode. After excitation had been achieved, forcing was stopped and the subsequent free oscillation motion of the fluid was recorded. Under these conditions the fluid motion was almost entirely that of the slosh mode and thereby could be used to determine the slosh mode frequency. To eliminate system noise error for this case the bridge output was subjected to a frequency filter before it was recorded.

For both the slosh mode and the pendulum-tank mode, the frequency for each pivot-point location and fluid height was determined three times. Repeatability was within 1 percent or better. Since an average of the three readings was used, the experimental error is estimated to be 1/2 percent or better.

### Range of Data and Sources of Error

To check the effect of fluid height on experimental-analytical correlation, tests were performed over an  $h/a$  (ratio of fluid height to tank radius) range of 0.50 to 2.00. For each  $h/a$  value an  $l$  (distance from pivot point to empty-tank cg) range of roughly 0.6 to 2.5 inches was tested to indicate the relative effects of rotation and

translation upon the correlation. For the smallest  $l$  and largest  $h/a$  values tested ( $l = 0.594$  in.,  $h/a = 2.00$ ), a 1/10-inch transverse displacement of the undisturbed fluid center of gravity corresponded to an angular rotation of  $3.77^\circ$ . For the largest  $l$  and smallest  $h/a$  value tested ( $l = 2.469$  in.,  $h/a = 0.50$ ) the same transverse displacement corresponded to an angular deviation of  $0.90^\circ$ . Free oscillations were started from an initial pendulum-tank angle of around  $10^\circ$ , which was small enough to prevent splashing.

The possible sources of error pertain, of course, to the quantities used to correlate experimental and analytical results, namely, the frequencies of the slosh mode (mostly fuel motion) and the pendulum-tank mode (mostly tank motion), together with the wave form of the two measured coordinates.

One source of error arises from the fact that damping was neglected in the analysis. Hence only qualitative wave form correlation would be expected on the time histories. On the other hand, in analogy to a linear one-degree-of-freedom system, slight damping would not change the modal natural frequencies appreciably. A computation using the observed damping factor indicated a natural frequency change of less than 1 part in  $10^4$ , well within the estimated maximum experimental error of 1/2 percent.

The capacitive probe contributed two possible errors in the determination of the fluid motion, namely noise and the tendency of the fluid to stick to the probe. These effects increased the difficulty experienced in wave-form correlation for the fluid motion but had no effect on the frequency determination.

The possible frequency error from recorder paper speed was checked by a precision frequency generator. Indicated error from this source was less than 1 part in 2000. This check was made for both the analog computer and experimental data recorders. Possible frequency error from filtered traces was determined by comparison with nonfiltered traces where possible. All such checks indicated deviations within the estimated maximum experimental error. In a similar fashion manually excited slosh mode frequencies were checked against the same frequencies as determined from quiescent initial conditions. Again deviations were within the outer limit of 1/2 percent arrived at from the repeatability check and the averaging procedure.

#### Analytical Models and Methods

In the appendix it is shown that both the pendulum model and the spring-bob model can be made to duplicate exactly the tank-surface forces and moments due to forced lateral translation and pitching of a partially filled cylindrical tank (shown in fig. 2) as predicted by linearized hydrodynamic theory. These models (pictured in figs. 3(a) and 3(b)) can,

of course, be used to determine parameters for the analytical simulation of free vibrations of the pendulum tank considered in the present report. Figure 4(a) shows this tank simulation for the case where a single pendulum of length  $L_1$  and mass  $m_1$ , and a fixed mass  $m_0$  with rotary inertia  $I_0$ , are used as a fuel model. The remainder of figure 4(a) is self-explanatory except for the fact that the figure utilizes the following identities between the pendulum and spring-bob models taken from equations (A19), (A20), (A22), and (A23) of the appendix for  $n = N = 1$ :

$$\begin{aligned} m_{1s} &= m_{1p} \equiv m_1 & l_{os} &= l_{op} \equiv l_o \\ m_{os} &= m_{op} \equiv m_o & I_{os} &= I_{op} \equiv I_o \end{aligned}$$

where the symbols are defined under Notation. It should be noted that  $\phi_1$  is proportional to the relative fluid motion in the first mode.

With  $b$  for effective gravity, and  $M$  and  $I$  denoting the mass and hinge-line moment of inertia of the pendulum tank without fuel, the following two linearized equations of motion can be derived for the system of figure 4(a) by Lagrange's equations or direct application of force balance:

$$L_1 \ddot{\phi}_1 + (l_{fp} + L_1) \ddot{\theta} + b(\phi_1 + \theta) = 0 \quad (1)$$

$$(I + I_o + m_o l_t^2 + m_1 l_{fp}^2) \ddot{\theta} + m_1 l_{fp} L_1 (\ddot{\phi}_1 + \ddot{\theta}) + b(Ml + m_o l_t + m_1 l_{fp}) \theta = 0 \quad (2)$$

Figure 4(b) shows the case where a single spring-bob of stiffness  $k_1$  and mass  $m_1$  replaces the pendulum in the fuel model. The two linearized equations of motion are as follows:

$$\ddot{s}_1 - \ddot{\theta} l_{fs} + \frac{k_1}{m_1} s_1 - b\theta = 0 \quad (3)$$

$$(I + I_o + m_o l_t^2 + m_1 l_{fs}^2) \ddot{\theta} - m_1 l_{fs} \ddot{s}_1 + b(Ml + m_o l_t + m_1 l_{fs}) \theta - m_1 b s_1 = 0 \quad (4)$$

where  $s_1$  is the relative displacement shown in figure 4(b).

Since the pendulum and spring-bob models must produce the same tank surface forces and moments on a mode-by-mode basis in order to duplicate the same hydrodynamic theory, it is expected that the linearized equations (3) and (4) can be converted to equations (1) and (2) by a simple linear transformation between  $s_1$  and  $\phi_1$ . This expectation is borne out when the substitution

$$s_1 = -L_1 \phi_1 \quad (5)$$

is made in equations (3) and (4), together with the identities (A21), (A8), (A14), and (A19) from the appendix for  $n = N = 1$ . Hence equations (1) and (2) were used interchangeably with equations (3) and (4) for the analysis. Occasionally both sets were used as a check on the analytical frequencies and wave forms.

After the parameters for equations (1) and (2) or equations (3) and (4) were specified numerically as described in the next subsection, analytical frequencies were determined by extracting roots from the characteristic determinant of these equations. For convenience in plotting the time histories, the equations were also set up on an analog computing machine and subjected to an initial displacement in  $\theta$ , with a corresponding initial  $\phi_1$  or  $s_1$  determined by static equilibrium. These initial displacements, together with zero initial velocities, correspond to the experimental initial conditions described in a previous subsection.

#### Numerical Determination of Analytical Parameters

The numerical parameters of table I were used for equations (1) and (2) (and various identities from the appendix for  $n = N = 1$  would give immediate conversion if parameters for equations (3) and (4) were desired).

The value given in table I for the fixed mass  $M$  of the empty pendulum tank was measured directly, of course, and  $b$  was taken as the sea-level acceleration due to gravity. Different fluid heights  $h$  and various pivot-point locations were selected to determine the two parameters,  $h/a$  and  $l$ , which are considered independent variables in table I. The tank radius  $a$  was measured directly, and  $l$  was determined by balancing the empty pendulum tank horizontally on a knife edge for each pivot-point location and measuring the distance from the pivot point to the knife edge. For each value of  $h/a$ , the corresponding value of  $L_1$  was determined from equation (A8) in the appendix with  $\epsilon_1 = 1.84119$  (ref. 14). Also for each  $h/a$ , the total fluid mass  $m$  was measured, and this permitted the determination of  $m_1$ ,  $m_0$ , and  $I_0$  by equations (A9), (A7), and (A13), respectively. For each value of  $l$ , the hinge-line moment of inertia  $I$  of the empty pendulum tank was determined by its measured natural frequency. Finally, for each combination of  $l$  and  $h/a$ , the distance  $l_m$  from the hinge line of the pendulum tank to the center of gravity of the undisturbed fluid was measured, and this was used with equations (A10) and (A11) and the length identities indicated in figure 4(a) to determine the values of  $l_{fp}$  and  $l_t$  given in table I.

## RESULTS AND DISCUSSION

### Comparison of Frequencies

A total of 28 combinations of  $l$  and  $h/a$  were used in this investigation. The slosh-mode and pendulum-tank-mode experimental and analytical frequencies are presented in table II. For this set the maximum deviation of an analytical from experimental modal frequency was 2.9 percent. Ninety percent of the frequencies had deviations of 1 percent or less; 70 percent had deviations of 0.5 percent or less; and 40 percent had deviations of 0.2 percent or less.

It should be noted that the frequencies discussed above are for the normal (combined) modes of a two-degree-of-freedom system in which coupling between the pristine modes (as designated herein) occurs. For the present system the latter consists of one mode in which the tank is held fixed while the fluid is in motion and a second mode in which the tank moves with the fluid frozen inside. What has been called the slosh mode is actually a combination of the two pristine modes in which the moving fluid component is predominant. Similarly, the pendulum-tank mode is a combination in which the tank plus frozen fluid component predominates.

Since the pristine modes are independent of all the fuel model parameters except those giving fluid natural frequencies, any free oscillation test of all the parameters requires that the coupling (resulting from fluid-tank force and moment interactions) described above be present. Furthermore for the test to be adequate the coupling effects must be sizable. The simplest measure of coupling in a system is the change in coupled modal frequency from pristine modal frequency. Computations revealed that for the present test such frequency changes ranged from 0.5 to 44 percent, with a roughly linear distribution for intermediate states. This indicates that enough data points with sizable coupling effects have been included to make the test significant; and the test then has the special advantage of determining how the analytical sloshing parameters perform when a combination of modes is present, as in an actual missile.

### Comparison of Time-History Wave Forms

For a qualitative comparison of time-history wave forms, three sets of unfiltered analytical-experimental traces are shown in figure 5. These are representative of the various qualitative features used in the correlation. In figure 5(a) the  $\theta$  trace exhibits beating, with experimental and analytical beat frequencies nearly equal. The corresponding traces for  $\phi_1$  and fluid height do not exhibit features as outstanding as the smooth beating just described. The wave-form correlation here is poor. It should be noted that the experimental traces for fluid height required

larger amplitudes of tank motion than did the corresponding  $\theta$  traces. It is possible that these amplitudes introduced nonlinearities which, with the damping of the system and the limitations of the capacitive probe, made wave form correlation poor or indecisive for all fluid traces except the most outstanding.

An example of outstanding wave-form correlation between  $s_1$  (note in eq. (5) that  $s_1 = -L_1\phi_1$ ) and fluid height is shown in figure 5(b). Here the easily correlated feature of one frequency component visibly superposed on the second is present. The result is a series of irregular peaks and valleys that can be followed on both the analytical and experimental traces for several cycles. The observable noise has been discussed earlier. The accompanying  $\theta$  coordinate is featureless in this instance.

Figure 5(c) represents a state of the system intermediate between the preceding two. Here the  $\theta$  trace exhibits "snaking," or more precisely, a low-frequency oscillation of the mean line for the most immediately apparent sinusoidal wave. The wave form agreement here is quite good. The corresponding  $\phi_1$  and fluid height traces are not particularly distinguishable, but both do display the same general peak-to-peak variations.

On the average, an analytical time history duplicated the corresponding experimental coordinate time history for 4 cycles, with general agreement continuing indefinitely.

## CONCLUSIONS

An experimental evaluation has been presented for specific analytical models for the stiffness and inertia terms of fuel sloshing in circular cylindrical tanks. The evaluation is based on two-degree-of-freedom analytical predictions, with sloshing represented by a single pendulum or spring-bob, of the experimental frequencies and wave forms for small, free oscillations of a smooth-walled pendulum tank containing mercury. The following conclusions are indicated:

1. In view of the maximum error between experiment and analysis of 2.9 percent for all slosh and pendulum tank frequencies, the maximum error of 0.5 percent for 70 percent of those frequencies, and the surprisingly good correlation of the time-history wave forms despite the damping of the physical system, it is concluded that either the pendulum or the spring-bob model provides excellent simulation of the stiffness and inertia terms for fuel sloshing.

2. The well-known identity between pendulums and spring-bobs for small oscillations is maintained in their rather complicated simulation of tank-surface forces and moments given by linearized hydrodynamic theory for a partially filled cylindrical tank undergoing small lateral and pitching oscillations, and this simulation is exact.

Ames Research Center

National Aeronautics and Space Administration

Moffett Field, Calif., Feb. 16, 1961

## APPENDIX A

DEVELOPMENT AND COMPARISON OF ANALYTICAL MODELS FOR  
FORCED LATERAL AND PITCHING OSCILLATIONS OF A  
PARTIALLY FILLED CYLINDRICAL TANK

FORCES AND MOMENTS ON TANK SURFACE

The method for developing analytical models for forced lateral translation and pitching of a partially filled cylindrical fuel tank is to determine masses and locations of pendulums or spring-bobs so as to match forces and moments on the tank surface, which are known from exact linearized hydrodynamic theory for inviscid fluids. The exact results, which can be derived by application of linearized boundary conditions to the Laplace equation as in reference 14, are presented below, with symbols defined under Notation and in figure 2:

$$F_x = \omega^2 x_o e^{i\omega t_m} \left[ 1 + \frac{2}{h} \sum_{n=1}^{\infty} \frac{\tanh\left(\epsilon_n \frac{h}{a}\right)}{\epsilon_n (\epsilon_n^2 - 1) \left(\frac{\omega_n^2}{\omega^2} - 1\right)} \right] \quad (A1)$$

$$M_x = \omega^2 x_o e^{i\omega t_m} \left[ \frac{1}{4} \frac{h}{a} + \sum_{n=1}^{\infty} \frac{\tanh\left(\epsilon_n \frac{h}{a}\right) + \frac{4}{\left(\epsilon_n \frac{h}{a}\right) \cosh\left(\epsilon_n \frac{h}{a}\right)} - \frac{2}{\epsilon_n \frac{h}{a}}}{\epsilon_n (\epsilon_n^2 - 1) \left(\frac{\omega_n^2}{\omega^2} - 1\right)} \right] \quad (A2)$$

$$F_\theta = m b \theta_o e^{i\omega t} + 2\omega^2 \theta_o e^{i\omega t_m} \left[ \frac{1}{8} \frac{h}{a} + \sum_{n=1}^{\infty} \frac{\frac{2}{\epsilon_n \frac{h}{a} \cosh\left(\epsilon_n \frac{h}{a}\right)} - \frac{1}{\epsilon_n \frac{h}{a}} + \frac{\tanh\left(\epsilon_n \frac{h}{a}\right)}{2}}{\epsilon_n (\epsilon_n^2 - 1) \left(\frac{\omega_n^2}{\omega^2} - 1\right)} \right] \quad (A3)$$

$$M_\theta = mab \frac{1}{4} \frac{h}{a} \theta_0 e^{i\omega t} + \omega^2 \theta_0 e^{i\omega t} m a^2 \left\{ \frac{1}{12} \left( \frac{h}{a} \right)^2 - \frac{1}{2} + A + 2 \sum_{n=1}^{\infty} \frac{1}{\epsilon_n (\epsilon_n^2 - 1) \left( \frac{\omega_n^2}{\omega^2} - 1 \right)} \left[ \frac{2}{\epsilon_n \cosh \left( \epsilon_n \frac{h}{a} \right)} - \frac{1}{\epsilon_n} - \tanh \left( \epsilon_n \frac{h}{a} \right) \left( \frac{4}{\epsilon_n^2 \frac{h}{a}} - \frac{\frac{h}{a}}{4} \right) - \frac{4}{(\epsilon_n^2) \frac{h}{a} \sinh \left( \epsilon_n \frac{h}{a} \right)} + \frac{5}{(\epsilon_n^2) \frac{h}{a} \tanh \left( \epsilon_n \frac{h}{a} \right)} \right] \right\} \quad (A4)$$

where

$$A = \frac{2}{a} \sum_{n=1}^{\infty} \frac{-4 + 5 \cosh \left( \epsilon_n \frac{h}{a} \right)}{\epsilon_n^3 (\epsilon_n^2 - 1) \sinh \left( \epsilon_n \frac{h}{a} \right)} \quad (A5)$$

and the pristine slosh frequencies  $\omega_n$  are given by

$$\omega_n^2 = \frac{b}{a} \epsilon_n \tanh \left( \epsilon_n \frac{h}{a} \right), \quad n = 1, 2, \dots, \infty \quad (A6)$$

These particular arrangements of the exact hydrodynamic results are important for matching with pendulums or spring-bobs. For that purpose  $\omega$  should enter within a summation only in modal coefficients of  $1/[(\omega_n^2/\omega^2) - 1]$ , and everything which is not such a coefficient should be taken out of the summation and regarded as a summed number. Then the modal coefficients can be compared with those of the pendulums or spring-bobs on a mode-by-mode basis.

#### PENDULUM MODEL

The pendulum model is shown in figure 3(a). For a total of  $N$  pendulums, giving  $N$  fluid modes, the following requirement is imposed:

$$m = m_{Op} + \sum_{n=1}^N m_{np} \quad (A7)$$

Determination of the model requires solution for the unknowns  $L_n$ ,  $m_{np}$ ,  $m_{op}$ ,  $l_{np}$ ,  $l_{op}$ , and  $I_{op}$ . With the well-known formula for the natural frequency of a simple pendulum, equation (A6) yields immediately

$$L_n = \frac{a}{\epsilon_n \tanh\left(\epsilon_n \frac{h}{a}\right)}, \quad n = 1, 2, \dots, N \quad (A8)$$

The first major step in solving for the remaining unknowns is to match  $F_x$  and  $M_x$  for forced lateral motion of the tank of figure 3(a) at  $x = x_0 e^{i\omega t}$ , positive right. The linearized equation of motion for  $m_{np}$  is (with  $\phi_{xn}$  defined in the Notation)

$$m_{np}(L_n \ddot{\phi}_{xn} + \omega_n^2 x_0 e^{i\omega t}) + m_{np} b \phi_{xn} = 0$$

and solution for  $\phi_{xn}$  gives  $F_{xnp}$ , the contribution of the  $n$ th pendulum to the wall force  $F_{xp}$ , by

$$F_{xnp} = -m_{np} b \phi_{xn}, \quad n = 1, 2, \dots, N$$

It is evident that for the fixed mass the force on the tank wall is

$$F_{xop} = m_{op} \omega^2 x_0 e^{i\omega t}$$

and after a little algebra  $F_{xp}$  is given by

$$F_{xp} = F_{xop} + \sum_{n=1}^N F_{xnp} = m \omega^2 x_0 e^{i\omega t} \left( 1 + \sum_{n=1}^N \frac{m_{np}}{m} \frac{1}{\frac{\omega_n^2}{\omega^2} - 1} \right)$$

A mode-by-mode comparison of  $F_{xp}$  with  $F_x$  of equation (A1) gives

$$m_{np} = \frac{2m \tanh\left(\epsilon_n \frac{h}{a}\right)}{\epsilon_n (\epsilon_n^2 - 1) \frac{h}{a}} \quad (A9)$$

and equation (A7) can be used to solve for  $m_{op}$ .

It is apparent from figure 3(a) that for forced translation the tank-surface moment  $M_{xp}$  must have the following components:

$$M_{xnp} = -l_{np} F_{xnp}$$

$$M_{xop} = -l_{op} F_{xop}$$

Then

$$M_{xp} = M_{xop} + \sum_{n=1}^N M_{xnp}$$

and when the algebra is worked out, a mode-by-mode comparison of  $M_{xp}$  with  $M_x$  of equation (A2) yields

$$\frac{l_{np}}{h} = - \left[ \frac{1}{2} + \frac{2}{\epsilon_n \frac{h}{a} \sinh\left(\epsilon_n \frac{h}{a}\right)} - \frac{1}{\epsilon_n \frac{h}{a} \tanh\left(\epsilon_n \frac{h}{a}\right)} \right] \quad (A10)$$

Comparison of the  $1/[4(h/a)]$  term of equation (A2) with the corresponding term of  $M_{xp}$  yields

$$\frac{l_{op}}{h} = - \sum_{n=1}^N \left[ \frac{m_{np}}{m_{op}} \frac{l_{np}}{h} - \frac{m}{m_{op}} \frac{1}{4\left(\frac{h}{a}\right)^2} \right] \quad (A11)$$

It is of some interest to note the sense in which equation (A11) preserves the center of gravity of the fluid. If  $L_n$  from equation (A8) is put in  $\sum_{n=1}^N (m_{np}/m_{op}) (L_n/h)$  and this quantity is added and subtracted on the right-hand side of equation (A11), some algebraic manipulation yields

$$m_{op} l_{op} + \sum_{n=1}^N m_{np} (l_{np} + L_n) = ma \left[ \frac{2}{\frac{h}{a}} \sum_{n=1}^N \frac{1}{\epsilon_n^2 (\epsilon_n^2 - 1)} - \frac{1}{4 \frac{h}{a}} \right]$$

If  $N \rightarrow \infty$ , it can be shown that  $\sum_{n=1}^{\infty} \frac{1}{\epsilon_n^2 (\epsilon_n^2 - 1)} = \frac{1}{8}$ , and thus in figure

3(a) the pendulums preserve the center of gravity of the fluid. Even for a single pendulum ( $N = 1$ ) the center of gravity is virtually maintained since the value of  $\epsilon_n$  for  $n = N = 1$  yields  $1/[\epsilon_1^2 (\epsilon_1^2 - 1)] = 1/8.1$ .

The second and final major step in developing the pendulum model of figure 3(a) is to match  $F_\theta$  and  $M_\theta$  for forced pitching of the tank about the center of gravity of the undisturbed fluid at  $\theta = \theta_0 e^{i\omega t}$ , positive clockwise. The linearized equation of motion for  $m_{np}$  is (with  $\varphi_{\theta n}$  defined in Notation)

$$m_{np}[L_n \ddot{\varphi}_{\theta n} - \omega^2(l_{np} + L_n)\theta_0 e^{i\omega t}] + b m_n(\varphi_{\theta n} + \theta_0 e^{i\omega t}) = 0 \quad (A12)$$

Again solution for  $\varphi_{\theta n}$  gives  $F_{\theta np}$ , the contribution of the  $n$ th pendulum to the wall force  $F_{\theta p}$ , by

$$F_{\theta np} = -m_{np} b \varphi_{\theta n}, \quad n = 1, 2, \dots, N$$

A combination of d'Alembert and gravity forces gives the force on the tank wall for the fixed mass as

$$F_{\theta op} = m_{op} b \theta_0 e^{i\omega t} - m_{op} l_{op} \omega^2 \theta_0 e^{i\omega t}$$

Then

$$F_{\theta p} = F_{\theta op} + \sum_{n=1}^N F_{\theta np}$$

and substitution of equations (A9), (A10), and (A11) gives an exact check of  $F_{\theta}$  in equation (A3) for all terms outside the modal summation and an exact mode-by-mode check within the summation. This result is strictly a check, of course, since no new unknowns are involved.

Figure 3(a) indicates that for forced pitching the tank-surface moment  $M_{\theta p}$  must have the following components:

$$M_{\theta np} = -l_{np} F_{\theta np}$$

$$M_{\theta op} = -l_{op} F_{\theta op} + \omega^2 I_{op} \theta_0 e^{i\omega t}$$

The use of equations (A9), (10), and (A11) in

$$M_{\theta p} = M_{\theta op} + \sum_{n=1}^N M_{\theta np}$$

then gives an exact mode-by-mode check within the modal summation of  $M_{\theta}$ , equation (A4), and also checks the term  $m a b \{1/[4(h/a)]\} \theta_0 e^{i\omega t}$ . The remaining terms are matched by the following solution for  $I_{op}$ :

$$I_{op} = \frac{m h^2}{12} + \frac{m a^2}{4} - m_{op} l_{op}^2 - \sum_{n=1}^N m_{np} l_{np}^2 + m a^2 \left( A - \frac{3}{4} \right) \quad (A13)$$

where  $A$  is the infinite summation of equation (A5). It should be noted that the first two terms of  $I_{op}$  give the moment of inertia of the fluid as if it were frozen. The solution for  $I_{op}$ , in terms of the quantities  $m_{np}$ ,  $m_{op}$ ,  $l_{np}$ , and  $l_{op}$  found earlier, completes the determination of the pendulum model of figure 3(a). These results agree with previous results found among references 11 to 13 when the latter are extended beyond  $N = 1$ .

## SPRING-BOB MODEL

The spring-bob model is shown in figure 3(b), and equation (A7) with subscripts  $s$  instead of  $p$ , is imposed as for the pendulum model. Determination of the spring-bob model requires solution for the unknowns  $k_n$ ,  $m_{ns}$ ,  $m_{os}$ ,  $l_{ns}$ ,  $l_{os}$ , and  $I_{os}$ . When the formula for the natural frequency of a spring-bob is combined with equation (A6),  $k_n$  can be found immediately in terms of  $m_{ns}$  as follows

$$k_n = m_{ns} \frac{b}{a} \epsilon_n \tanh\left(\epsilon_n \frac{h}{a}\right), \quad n = 1, 2, \dots, N \quad (A14)$$

The procedure in solving for the remaining unknowns is identical to that for the pendulum model. The following key equations in the development of the spring model replace corresponding equations in the pendulum development (see Notation and fig. 3(b) for definitions of symbols):

$$\begin{aligned} m_{ns}(\ddot{s}_{xn} - \omega^2 x_0 e^{i\omega t}) + k_n s_{xn} &= 0 \\ F_{xns} &= k_n s_{xn} \\ F_{xos} &= m_{os} \omega^2 x_0 e^{i\omega t} \\ M_{xns} &= -l_{ns} F_{xns} + m_{ns} b s_{xn} \\ M_{xos} &= -l_{os} F_{xos} \\ m_{ns}(\ddot{s}_{\theta n} + \omega^2 l_{ns} \theta_0 e^{i\omega t}) + k_n s_{\theta n} &= m_{ns} b \theta \\ F_{\theta ns} &= k_n s_{\theta n} \\ F_{\theta os} &= m_{os} b \theta_0 e^{i\omega t} - m_{os} l_{os} \omega^2 \theta_0 e^{i\omega t} \\ M_{\theta ns} &= -l_{ns} F_{\theta ns} + m_{ns} b s_{\theta n} \\ M_{\theta os} &= -l_{os} F_{\theta os} + \omega^2 I_{os} \theta_0 e^{i\omega t} \end{aligned}$$

From these equations the procedure followed for the pendulum model yields the following results to supplement equation (A7), with subscripts  $s$  instead of  $p$ , and equation (A14) for the spring-bob model:

$$m_{ns} = \frac{2m \tanh\left(\epsilon_n \frac{h}{a}\right)}{\epsilon_n (\epsilon_n^2 - 1) \frac{h}{a}} \quad (A15)$$

$$\frac{z_{ns}}{h} = - \left[ \frac{1}{2} + \frac{2}{\epsilon_n \frac{h}{a} \sinh\left(\epsilon_n \frac{h}{a}\right)} - \frac{2}{\epsilon_n \frac{h}{a} \tanh\left(\epsilon_n \frac{h}{a}\right)} \right] \quad (\text{A16})$$

$$\frac{z_{os}}{h} = - \left[ \sum_{n=1}^N \frac{m_{ns}}{m_{os}} \frac{z_{ns}}{h} + \frac{m}{\left(\frac{h}{a}\right)^2} \left[ 2 \sum_{n=1}^N \frac{1}{\epsilon_n^2 (\epsilon_n^2 - 1)} - \frac{1}{4} \right] \right] \quad (\text{A17})$$

$$I_{os} = \frac{mh^2}{12} + \frac{ma^2}{4} - m_{os} z_{os}^2 - \sum_{n=1}^N m_{ns} z_{ns}^2 + ma^2 \left[ A - \frac{3}{4} - 2 \sum_{n=1}^N \frac{1}{\epsilon_n^2 (\epsilon_n^2 - 1)} - \frac{2}{\frac{h}{a}} \sum_{n=1}^N \frac{4 - 3 \cosh\left(\epsilon_n \frac{h}{a}\right)}{\epsilon_n^3 (\epsilon_n^2 - 1) \sinh\left(\epsilon_n \frac{h}{a}\right)} \right] \quad (\text{A18})$$

where  $A$  is given in equation (A5).

As in the case of the pendulum model, the foregoing results for the spring-bob model duplicate the exact hydrodynamic forces and moments on the tank surface even for those terms whose duplication requires the use only of previously determined unknowns. When  $N \rightarrow \infty$ , the spring-bob results are identical to those of references 6 and 9. By the argument immediately following equation (A11), it is apparent that equation (A17) automatically preserves the fluid center of gravity as  $N \rightarrow \infty$  and very nearly does so for a single spring ( $N = 1$ ).

#### RELATIONS BETWEEN PENDULUM AND SPRING-BOB MODELS

Comparison of equations (A9) and (A15) shows

$$m_{ns} = m_{np} \equiv m_n, \quad n = 1, 2, \dots, N \quad (\text{A19})$$

where  $m_n$  is the symbol to be used for both models. Hence, by equation (A7) with subscripts  $p$  or  $s$ ,

$$m_{os} = m_{op} \equiv m_o \quad (\text{A20})$$

Comparison of equations (A10) and (A16), and use of equation (A8), yields

$$l_{ns} = l_{np} + L_n \quad (A21)$$

When equations (A21), (A8), and (A15) are introduced in equation (A17), it is found that

$$l_{os} = l_{op} \equiv l_o \quad (A22)$$

where  $l_o$  is the new symbol for both models. A similar operation on equation (A18), which involves lengthier algebra, yields

$$I_{os} = I_{op} \equiv I_o \quad (A23)$$

None of the above exact comparisons requires  $N \rightarrow \infty$ . In fact the  $n = 1$  term of all summations not involving the modal coefficient  $1/[(\omega_n^2/\omega^2) - 1]$  is completely dominant except as  $h/a \rightarrow 0$ . As  $h/a \rightarrow 0$ , the spring-bob forms in equations (A16) through (A18) are better for computational purposes than the corresponding pendulum forms since the hyperbolic sines and tangents in the denominator combine to give a half angle hyperbolic tangent in the numerator. For equation (A18) this combination requires  $N \rightarrow \infty$  since  $A$  of equation (A5) is an infinite summation. These computational matters are not too vital, however, since as  $h/a \rightarrow 0$  the fuel sloshing effect on stability disappears.

## REFERENCES

1. Cooper, R. M.: Dynamics of Liquids in Moving Containers. ARS Jour., vol. 30, no. 8, Aug. 1960, pp. 725-729.
2. Guthrie, F.: On Stationary Liquid Waves. Phil. Mag., series 4, vol. 50, 1875, pp. 290-302, 377-388.
3. Rayleigh, Lord: On Waves. Phil. Mag., series 5, vol. 1, no. 4, 1876, pp. 257-279.
4. Bauer, Helmut F.: Fluid Oscillation in a Cylindrical Tank with Damping. Army Ballistic Missile Agency, Tech. Rep. DA-TR-4-58, Apr. 23, 1958.
5. Abramson, H. Norman, and Ransleben, Guido E., Jr.: A Theoretical and Experimental Study of Fuel Sloshing. Quart. Progress Rep. No. 7, Southwest Research Institute, Feb. 1, 1960.
6. Abramson H. Norman, Chu, Wen-Hwa, and Ransleben, Guido E., Jr.: Representation of Fuel Sloshing in Cylindrical Tanks by an Equivalent Mechanical Model. Tech. Rep. No. 8, Southwest Research Institute, June 30, 1960.
7. Abramson, H. Norman, Ransleben, Guido E., Jr.: Simulation of Fuel Sloshing Characteristics in Missile Tanks by Use of Small Models. ARS Jour., vol. 30, no. 7, July 1960, pp. 603-612.
8. Graham, E. W., and Rodriguez, A. M.: The Characteristics of Fuel Motion Which Affect Airplane Dynamics. Jour. Appl. Mech., vol. 19, Sept. 1952, pp. 381-388.
9. Anderson, G. W.: Sloshing Parameters for Cylindrical Tanks. Rep. SM-37477, Douglas Aircraft Co., Inc., Santa Monica Div., Aug. 26, 1960.
10. Luskin, H., and Lapin, E.: An Analytical Approach to the Fuel Sloshing and Buffeting Problems of Aircraft. Jour. Aero. Sci., vol. 19, no. 4, Apr. 1952, pp. 217-228.
11. Kachigan, K.: Forced Oscillations of a Fluid in a Cylindrical Tank. Rep. ZU-7-046, Convair, San Diego, Oct. 4, 1955.
12. Schmitt, A. F.: Forced Oscillations of a Fluid in a Cylindrical Tank Undergoing Both Translation and Rotation. Rep. ZU-7-069, Convair, San Diego, Oct. 16, 1956.

13. Schmitt, A. F.: Forced Oscillations of a Fluid in a Cylindrical Tank Oscillating in a Carried Acceleration Field - A Correction. Rep. ZU-7-074, Convair, San Diego, Feb. 4, 1957.
14. Bauer, H. F.: Fluid Oscillations in a Circular Cylindrical Tank. Tech. Rep. DA-TR-1-58, Army Ballistic Missile Agency, Apr. 18, 1958.

TABLE I.- ANALYTICAL PARAMETERS

[Symbols are defined in the section on Notation]

$$M = 0.01167 \text{ lb sec}^2/\text{in.}$$

$$b = 386 \text{ in./sec}^2$$

h/a	$L_1$ , in.	$m_1$ , lb sec <sup>2</sup> /in.	$m_0$ , lb sec <sup>2</sup> /in.	$I_0$ , lb-in. sec <sup>2</sup>
1/2	1.454	0.00971	0.00499	0.00684
1	1.110	.01271	.01668	.00654
3/2	1.064	.01325	.03085	.00952
2	1.058	.01334	.04542	.02202

$z$ , in.	$I$ , lb-in. sec <sup>2</sup>
0.594	0.1174
.969	.1264
1.219	.1256
1.469	.1285
1.844	.1473
2.219	.1668
2.469	.1813

h/a z, in.	1/2		1		3/2		2	
	$z_{fp}$ , in.	$z_t$ , in.						
0.594	2.448	2.664	2.447	2.569	1.849	2.337	1.027	2.006
.969	2.948	3.164	2.947	3.069	2.349	2.837	1.527	2.506
1.219	3.448	3.664	3.447	3.569	2.849	3.337	2.027	3.006
1.469	3.948	4.164	3.947	4.069	3.349	3.837	2.527	3.506
1.844	4.448	4.664	4.447	4.569	3.849	4.337	3.027	4.006
2.219	4.948	5.164	4.947	5.069	4.349	4.837	3.527	4.506
2.469	5.448	5.664	5.447	5.569	4.849	5.337	4.027	5.006

TABLE II.- NATURAL FREQUENCIES FOR NORMAL (COMBINED) MODES

Slosh-mode frequencies, cps									
l	h/a = 0.50		h/a = 1.00		h/a = 1.50		h/a = 2.00		Analysis
	Experiment	Analysis	Experiment	Analysis	Experiment	Analysis	Experiment	Analysis	
0.594	3.269	3.177	3.563	3.563	3.333	3.352	3.138	3.150	3.150
.969	3.397	3.312	3.656	3.660	3.405	3.409	3.223	3.199	3.199
1.219	3.504	3.474	3.717	3.724	3.445	3.458	3.241	3.248	3.248
1.469	3.630	3.598	3.746	3.776	3.471	3.500	3.287	3.287	3.287
1.844	3.652	3.643	3.758	3.793	3.492	3.516	3.304	3.309	3.309
2.219	3.761	3.686	3.773	3.802	3.505	3.530	3.319	3.326	3.326
2.469	3.768	3.726	3.787	3.818	3.519	3.535	3.330	3.336	3.336
Pendulum-tank-mode frequencies, cps									
0.594	1.338	1.343	1.530	1.528	1.670	1.673	1.789	1.783	1.783
.969	1.355	1.353	1.494	1.461	1.620	1.619	1.727	1.725	1.725
1.219	1.345	1.343	1.452	1.454	1.564	1.572	1.665	1.657	1.657
1.469	1.328	1.324	1.405	1.408	1.495	1.496	1.590	1.578	1.578
1.844	1.298	1.291	1.357	1.353	1.435	1.429	1.504	1.499	1.499
2.219	1.255	1.254	1.308	1.311	1.371	1.372	1.435	1.433	1.433
2.469	1.225	1.222	1.267	1.265	1.318	1.335	1.372	1.372	1.372

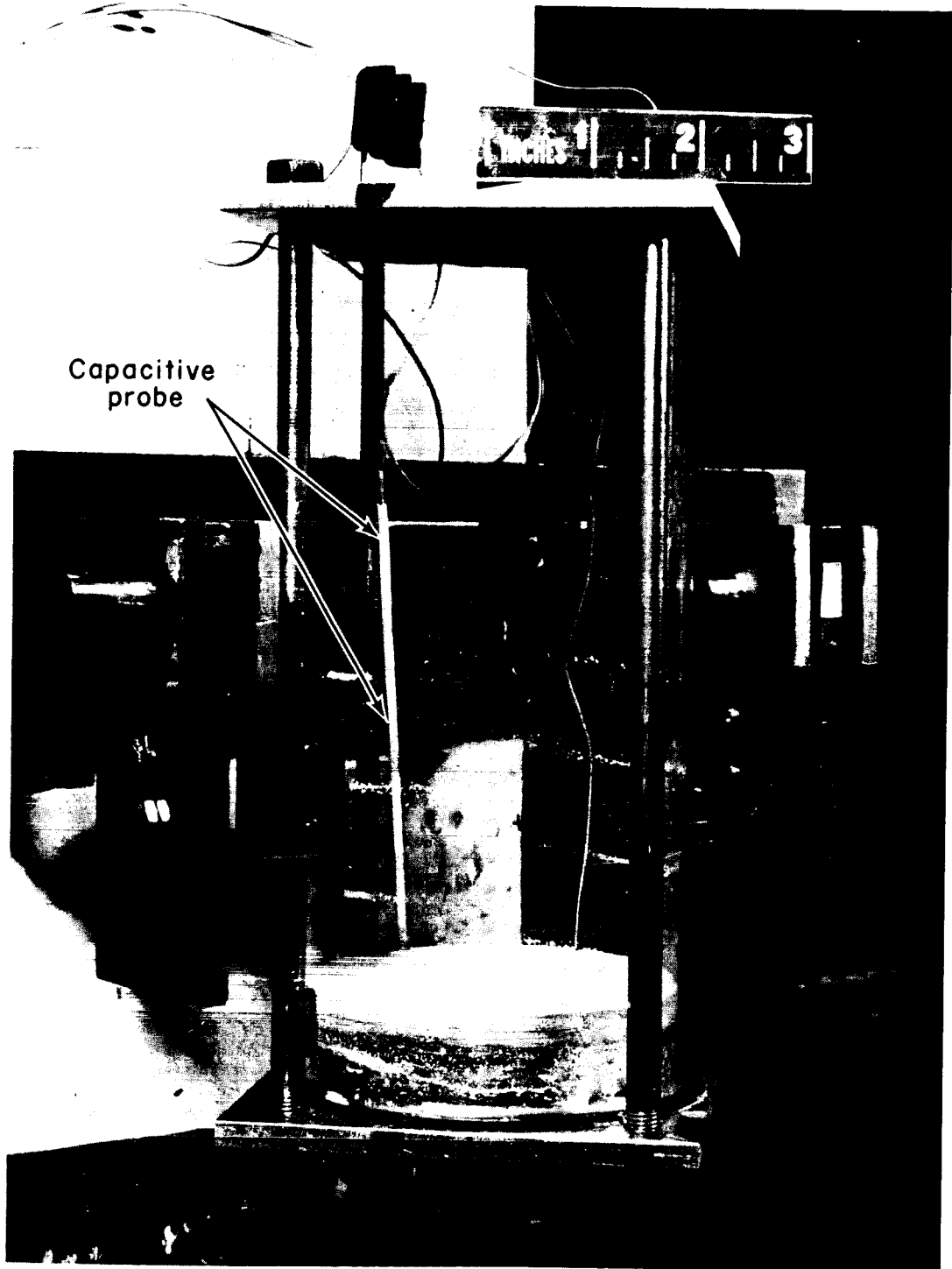


Figure 1.- Apparatus.

A-27013. 1

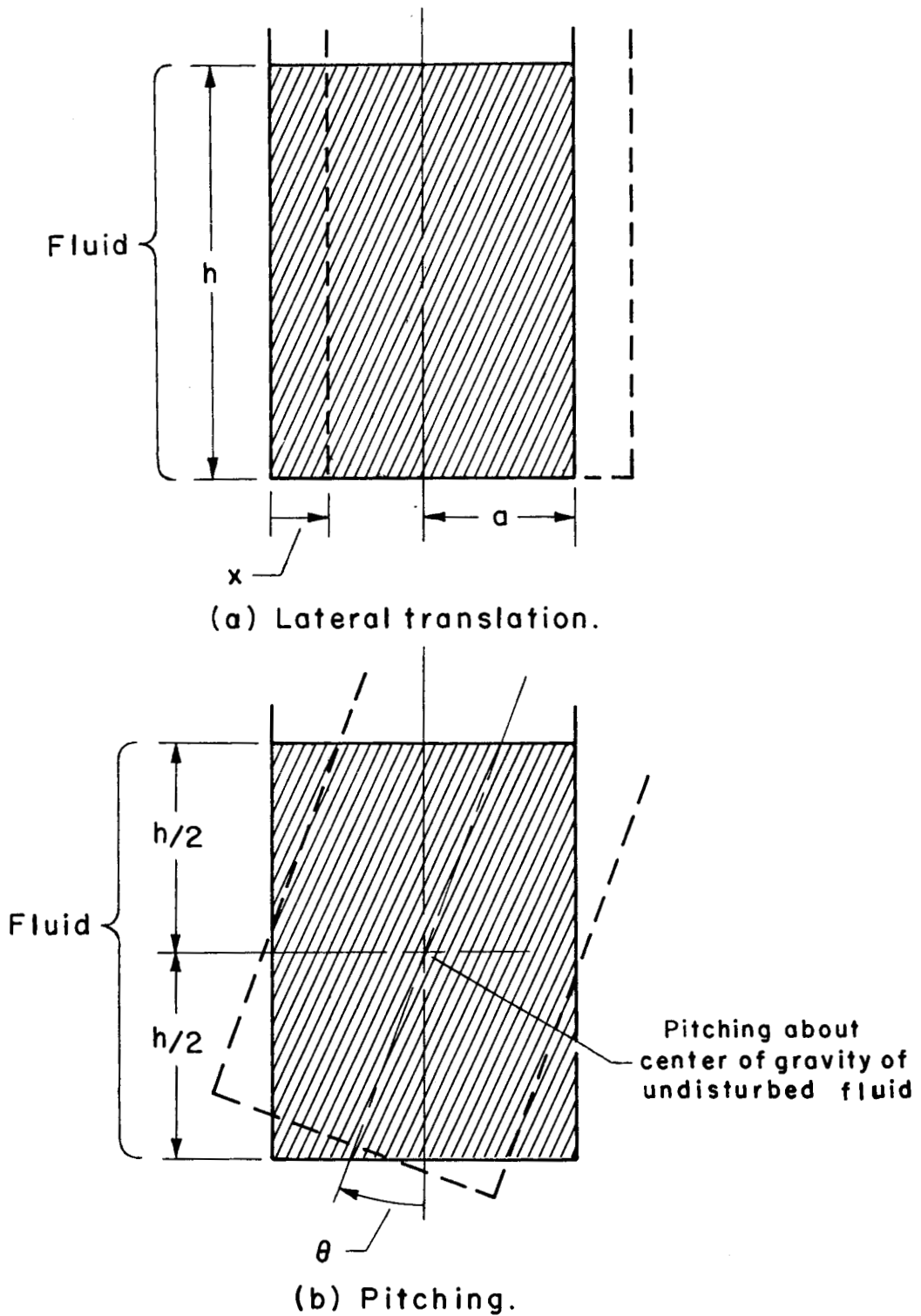


Figure 2.- Coordinates of partially filled cylindrical tank.

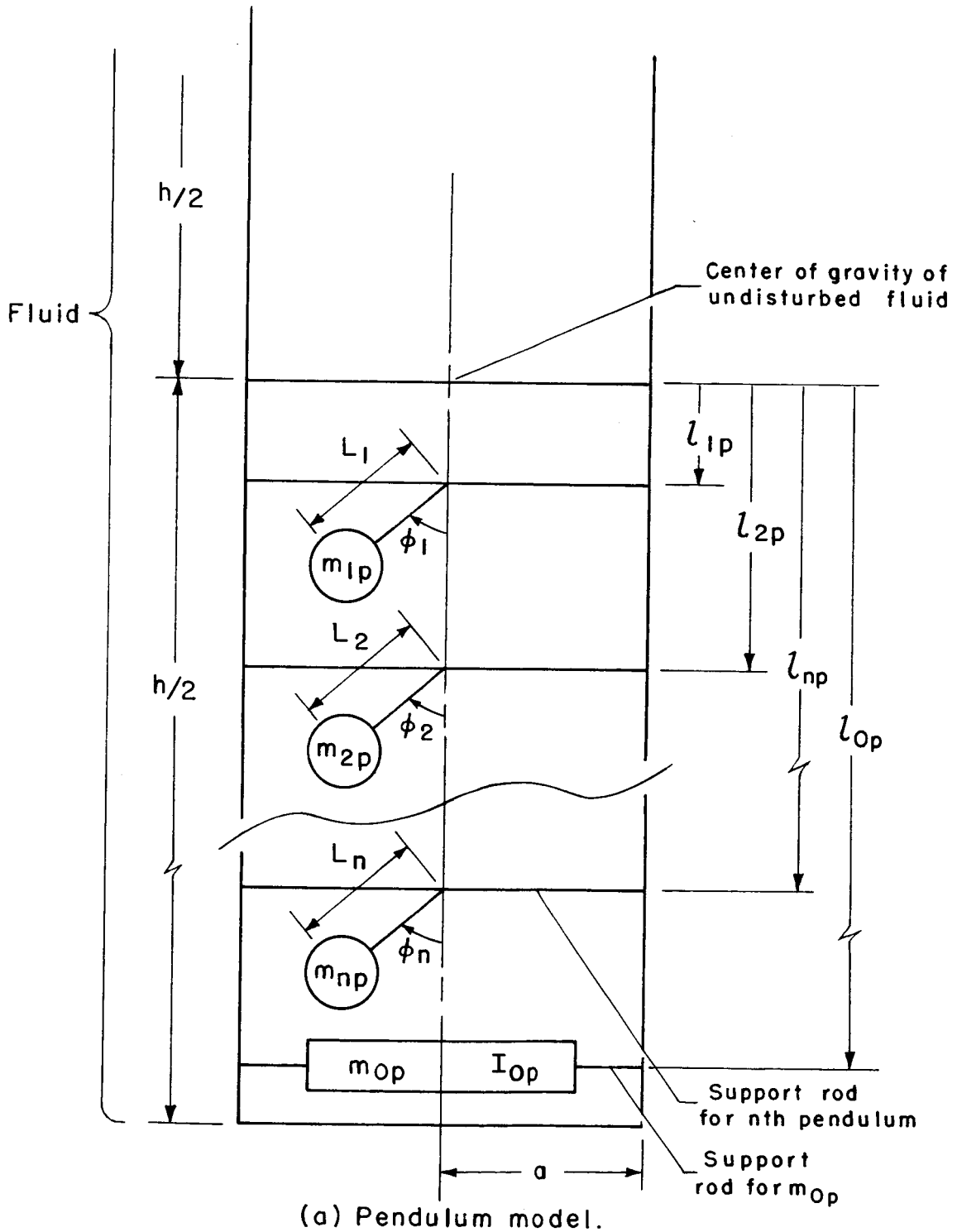
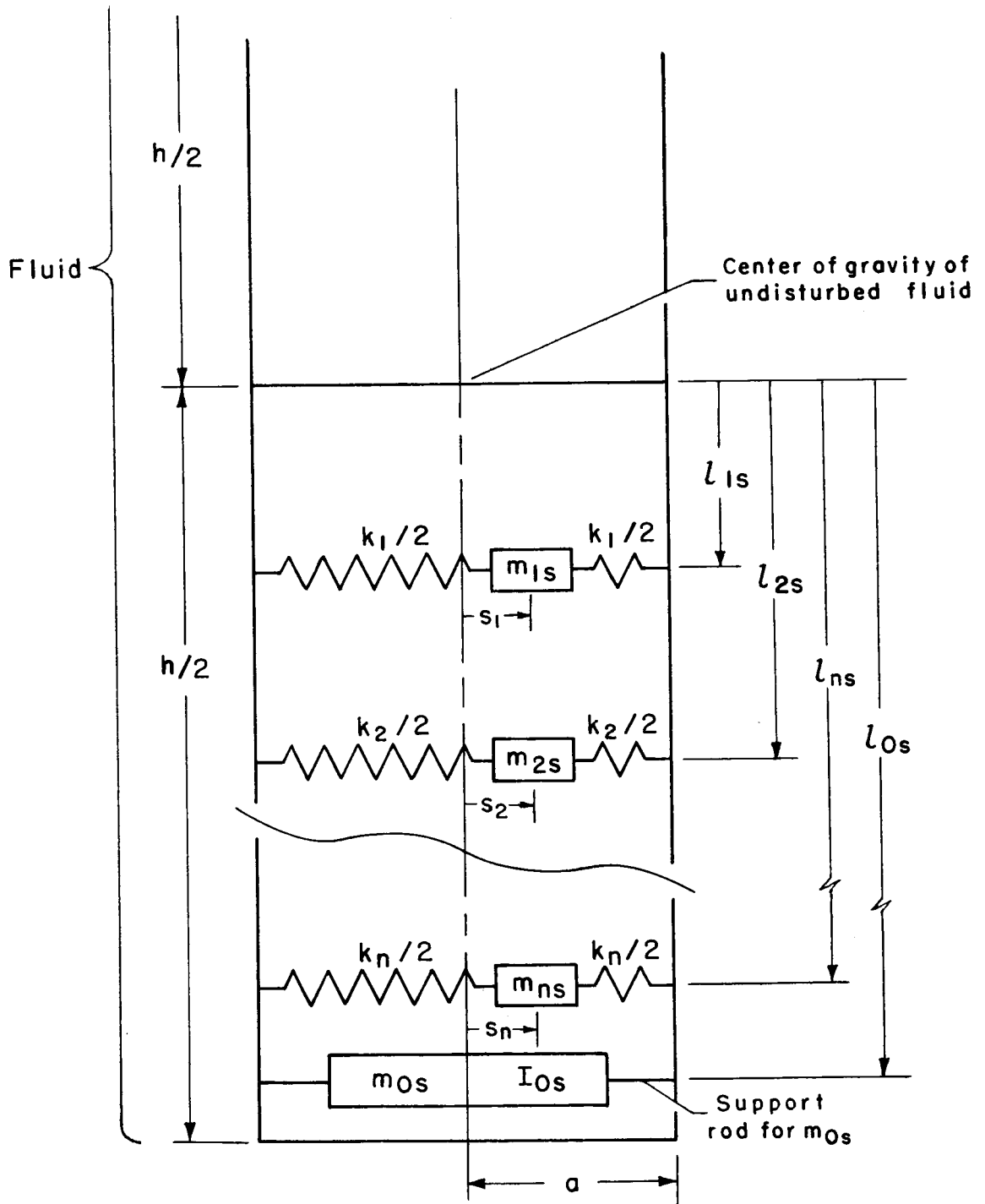
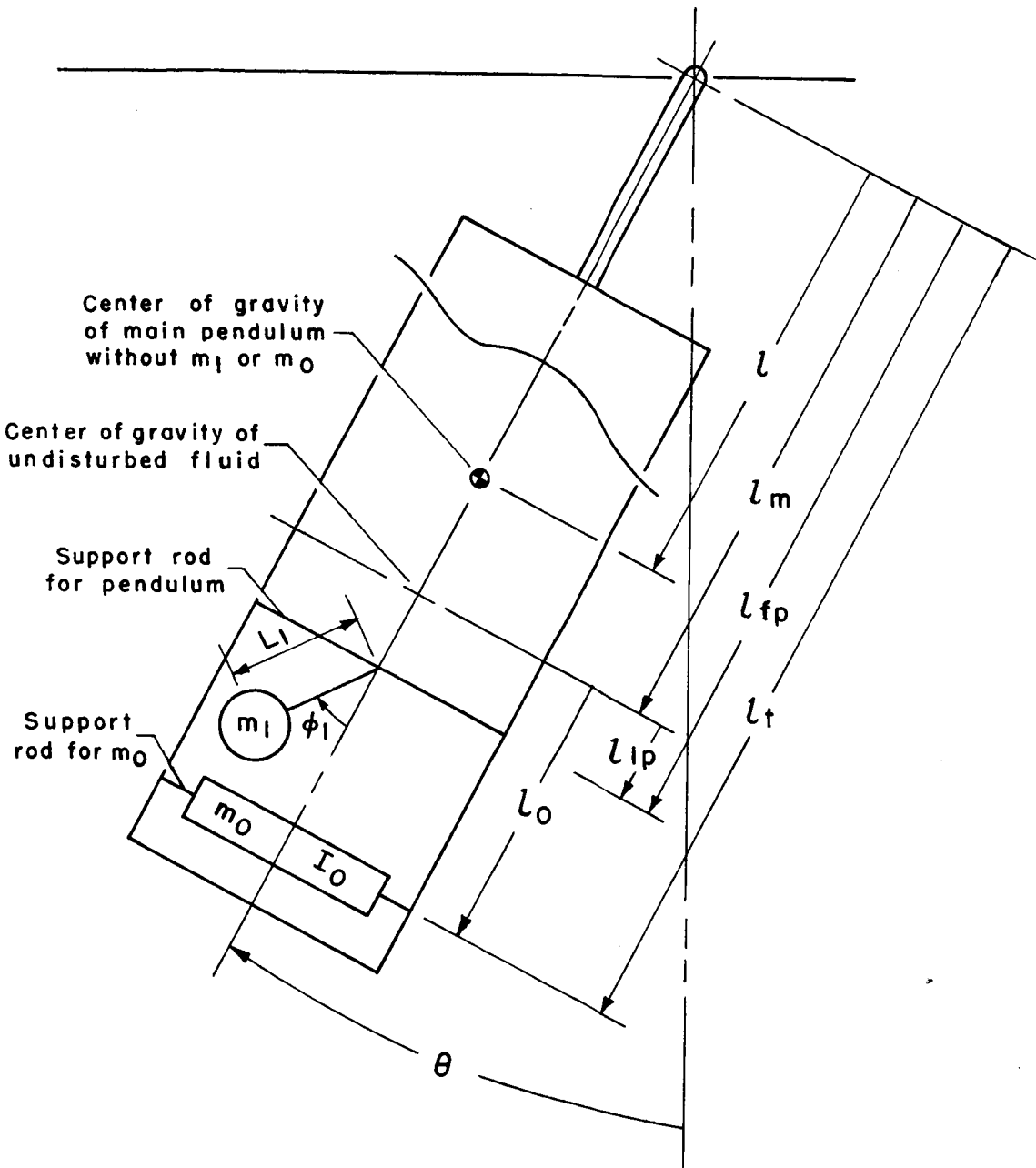


Figure 3.- Analytical models for forced translation and pitching of a partially filled cylindrical tank.



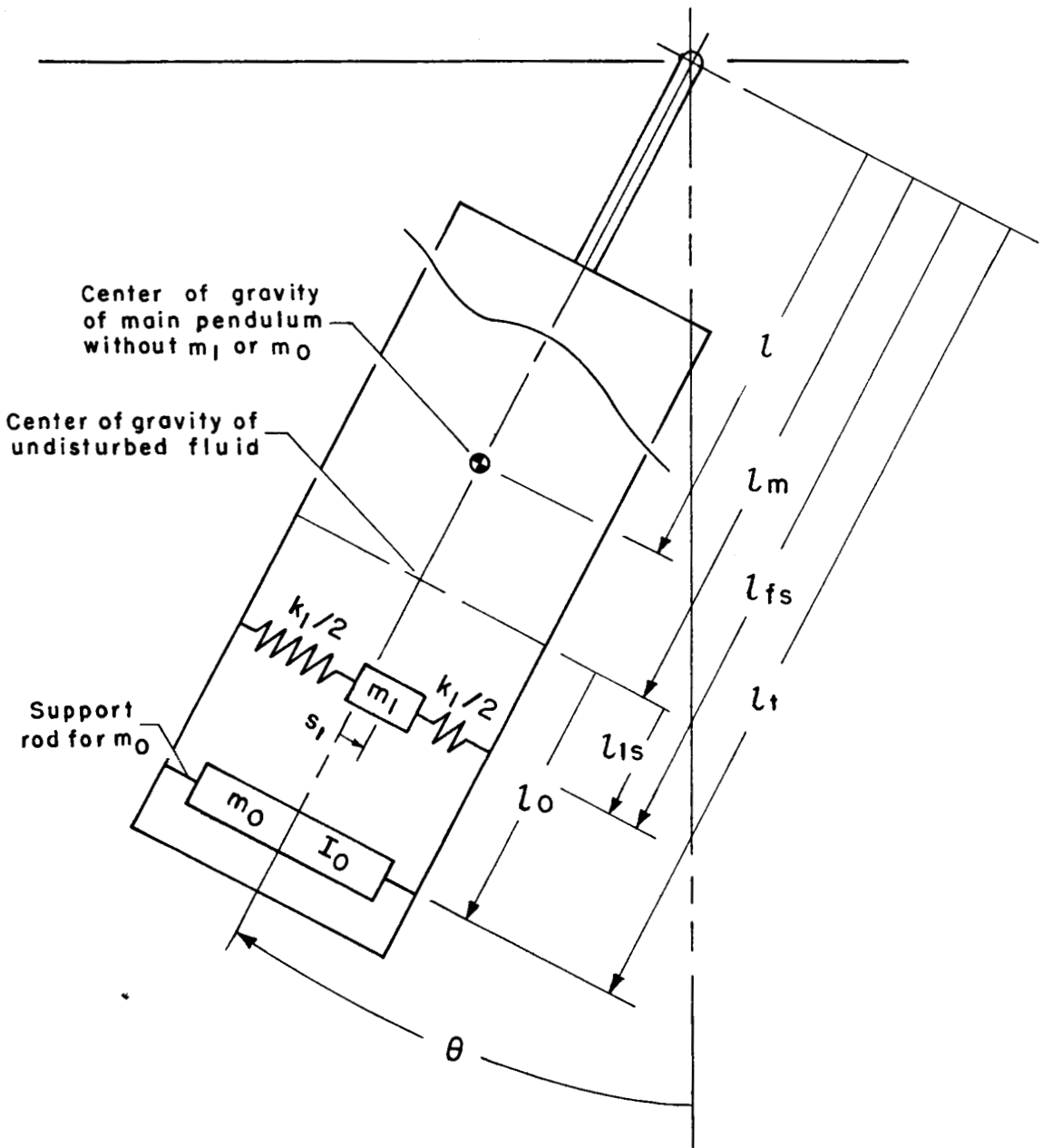
(b) Spring-bob model.

Figure 3.- Concluded.



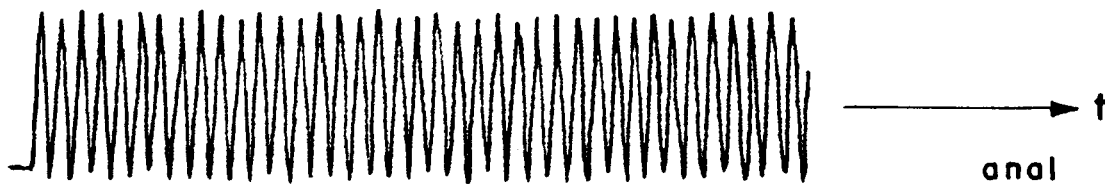
(a) Pendulum model for fuel.

Figure 4.- Analytical simulation for pendulum tank.

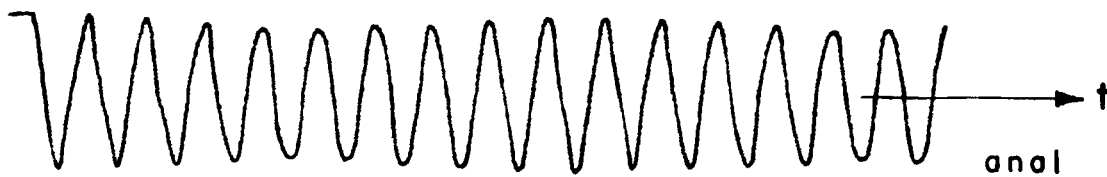
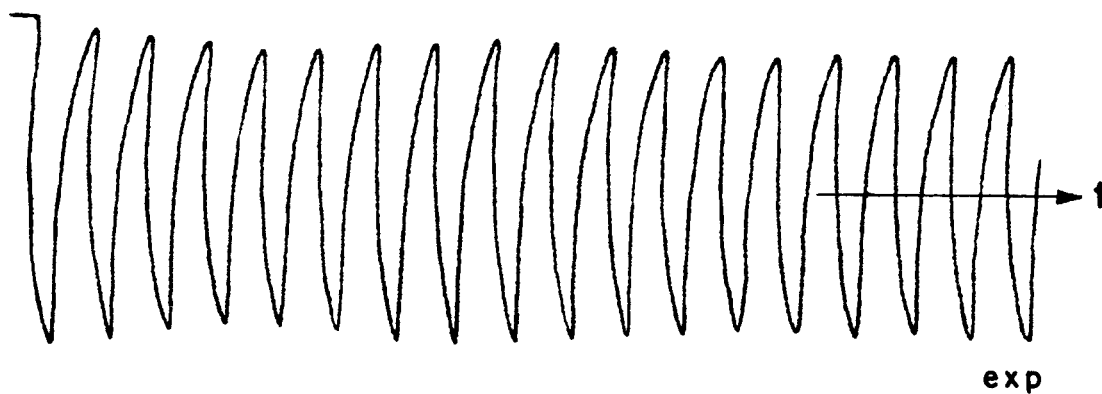


(b) Spring-bob model for fuel.

Figure 4.- Concluded.



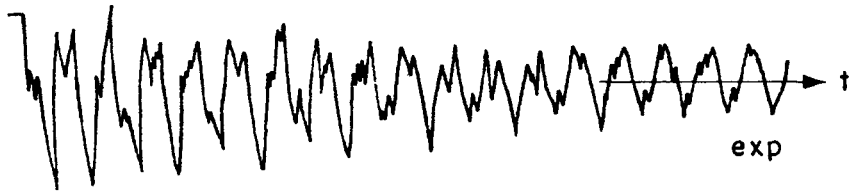
Ordinates are fluid height change at tank wall relative to tank bottom for the experiment and  $\phi_1$  for the analysis.



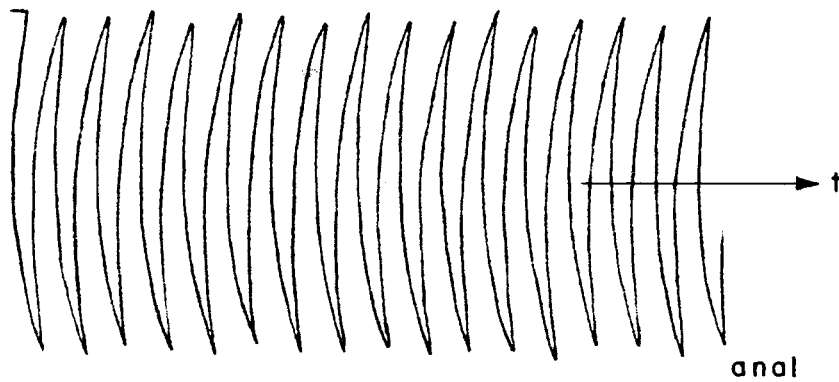
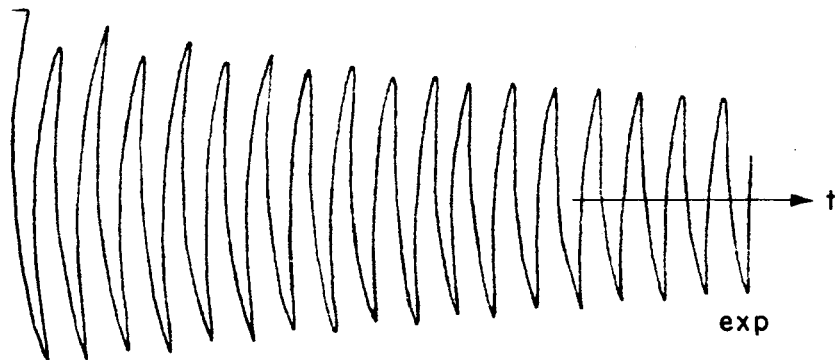
Ordinates are  $\theta$  for experiment and analysis.

(a)  $h/a = 1.00$ ,  $l = 2.219$  inches

Figure 5.- Sample experimental and analytical wave forms.



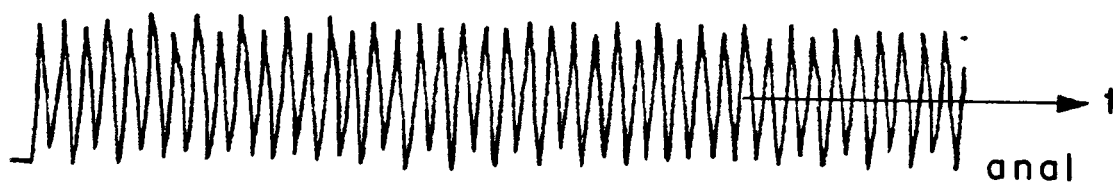
Ordinates are fluid height change at tank wall relative to tank bottom for the experiment and  $s_1$  for the analysis.



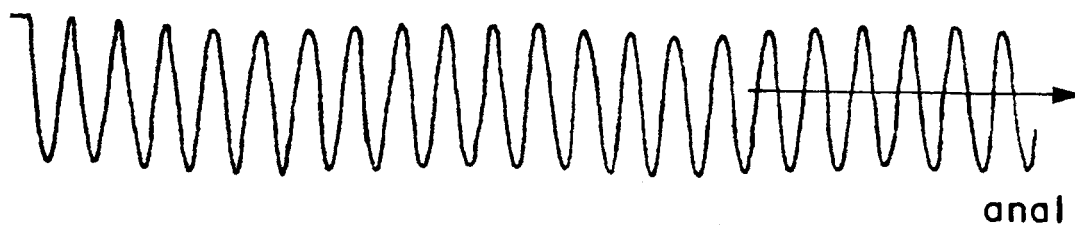
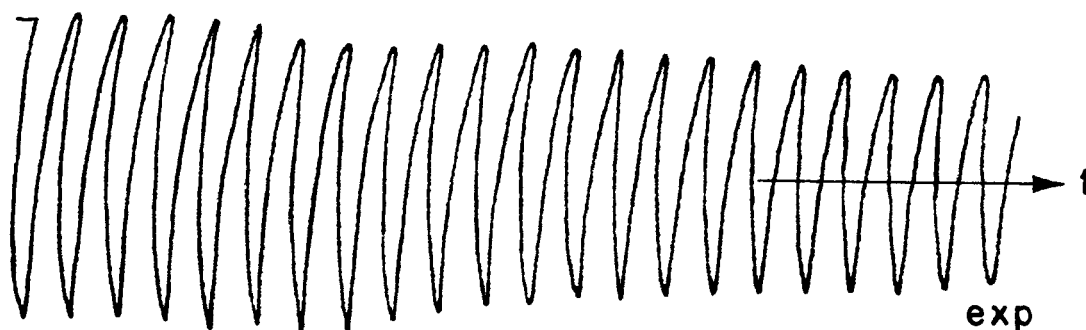
Ordinates are  $\theta$  for experiment and analysis.

(b)  $h/a = 0.50$ ,  $z = 0.594$  inch

Figure 5.- Continued.



Ordinates are fluid height change at tank wall relative to tank bottom for the experiment and  $\phi_1$  for the analysis.



Ordinates are  $\theta$  for experiment and analysis.

(c)  $h/a = 1.50$ ,  $l = 0.969$  inch

Figure 5.- Concluded.